Energy Conversion and Management 258 (2022) 115564

Contents lists available at ScienceDirect

Energy Conversion and Management

journal homepage: www.elsevier.com/locate/enconman

Adaptive ML-based technique for renewable energy system power forecasting in hybrid PV-Wind farms power conversion systems

Muhammad Hamza Zafar [a], Noman Mujeeb Khan [a], Majad Mansoor [b], Adeel Feroz Mirza [b], Syed Kumayl Raza Moosavi [c], Filippo Sanfilippo [d,*]

[a] Department of Electrical Engineering, Capital University of Science and Technology, Islamabad, Pakistan
[b] Department of Automation, University of Science and Technology of China, Hefei, China
[c] School of Electrical Engineering and Computer Science, National University of Science and Technology, Islamabad, Pakistan
[d] Department of Engineering Sciences, University of Agder, Grimstad, Norway

ARTICLE INFO

Keywords:
Power forecasting
Renewable energy resources (RES)
Improved dynamic group based cooperative (IDGC)

ABSTRACT

Large scale integration of renewable energy system with classical electrical power generation system requires a precise balance to maintain and optimize the supply–demand limitations in power grids operations. For this purpose, accurate forecasting is needed from wind energy conversion systems (WECS) and solar power plants (SPPs). This daunting task has limits with long-short term and precise term forecasting due to the highly random nature of environmental conditions. This paper offers a hybrid variational decomposition model (HVDM) as a revolutionary composite deep learning-based evolutionary technique for accurate power production forecasting in microgrid farms. The objective is to obtain precise short-term forecasting in five steps of development. An improvised dynamic group-based cooperative search (IDGC) mechanism with a IDGC-Radial Basis Function Neural Network (IDGC-RBFNN) is proposed for enhanced accurate short-term power forecasting. For this purpose, meteorological data with time series is utilized. SCADA data provide the values to the system. The improvisation has been made to the metaheuristic algorithm and an enhanced training mechanism is designed for the short term wind forecasting (STWF) problem. The results are compared with two different Neural Network topologies and three heuristic algorithms: particle swarm intelligence (PSO), IDGC, and dynamic group cooperation optimization (DGCO). The 24 h ahead are studied in the experimental simulations. The analysis is made using seasonal behavior for year-round performance analysis. The prediction accuracy achieved by the proposed hybrid model shows greater results. The comparison is made statistically with existing works and literature showing highly effective accuracy at a lower computational burden. Three seasonal results are compared graphically and statistically.

1. Introduction

Low-cost power generation and abundance of natural renewable energy resources enforce the integration of renewable and nonrenewable electrical power plants to be utilized simultaneously in national transmission grids. The most cost effective power generation is archived by wind and solar. Photovoltaic (PV) systems and wind energy conversion systems (WECS) power performance depends on volatile factors such as environmental conditions, base technology, and optimization. The most detrimental factor is the unpredictability of the total available power in a given time and its short-term forecasting. For instance, the wind speed vs. blade pitch angle and irradiance vs. power curves of the wind and solar show a nonlinear relationship. Alongside, high fluctuations are power generation tendencies along with the low magnitude of ideal operating conditions. The loss of available power from renewable sources has to be meet with cranking up nonrenewable power sources, which are also time-sensitive operations. Increased involvement of the European Union (EU), China, and the United states of America (USA) in renewable has pushed installed capacity of combined to 2799GW till the year 2020, with wind and solar providing 91% of the total increase of installed capacity [1]. Wind power forecasting is a difficult job since regional wind patterns in wind farms change and wind turbine reactions vary based upon turbine conditions. Forecasting wind output is critical for the successful integration of wind farms into the electricity system.

* Corresponding author.
E-mail address: filippo.sanfilippo@uia.no (F. Sanfilippo).

https://doi.org/10.1016/j.enconman.2022.115564
Received 19 January 2022; Received in revised form 20 March 2022; Accepted 28 March 2022
Available online 1 April 2022

At the actual time, the power output of a given wind energy conversion system can be calculated using: $P_W = \frac{1}{2}\rho \bullet \pi R_r^2 \bullet Cp \bullet w^3$, where the terms ρ, R_r and w are the density of air, the rotor radius, and the wind speed, respectively [2]. Theoretical power is highly affected by the rotor blade area and wind speed. Although the angle of attack of the turbine blade is controllable in real-time, the dominant effect of wind speed cannot be countered in seconds. To this end, 10 min to hours ahead prediction is needed to accommodate the increased or decreased utility of hybrid power generation units. The theoretical estimation of wind turbine power provides nonlinear s-shaped power characteristics curve logistic function for wind speed and density being an independent variable. However, due to the unpredictable nature of wind and the complex dynamics inside and between turbines, this equation does not perfectly represent the actual power production of individual wind turbines. A more realistic alternative model for each wind turbine in a farm may be produced by fitting measurements to actual data. The PV power throughout the year depends upon irradiance density, angle of elevation of the sun, changing weather and clouding patterns, cooling caused by wind, etc.

In addition to modelling hybrid PV-wind power generating mechanisms in response to operational conditions, wind farm managers must predict power based on present conditions. Recent research has employed complicated data-driven models, such as ANNs, to anticipate turbine production with some accuracy [3,4].

The main research gaps to investigate wind power forecasting are mentioned as below:

1. Primarily, deep neural network efficiency is strongly dependent on the hyper-parameter tuning optimization strategy. Nonetheless, the *meta*-heuristics used to enhance the hyper-parameters are frequently ineffective, because initializing the control parameters consumes a lot of time and is very challenging. Moreover, rather than fine-tuning hyperparameters on the target problem, the bulk of them have been modified based on numerical standards.
2. The parameter of decomposition Initialization is a critical function for achieving high efficiency. This initialization process is fraught with difficulties since insufficient setup options might jeopardize the predicting models' efficacy. Another disadvantage of such models is that the amount of processing time required grows drastically as the number of parameters grows.

This paper proposes an integrated methodology that combines ANNs with improvised DGCO for precise microgrid PV-Wind power forecasting. The input features used in current modeling are irradiance, temperatures, wind speed, wind direction, humidity, and theoretically available peak power.

Contributions of this work are as stated as follows:

1. Two-hybrid DL-based evolutionary intelligence-based frameworks (IDGC-RBN and IDGC-GRNN) are proposed for hybrid PV-wind power output prediction.
2. For outliers in SCADA data, complete data filtering is used, which is quite successful for seasonal behavior adjustment.
3. Performance of proposed models using SCADA datasets is compared comprehensively to quantify the ability of the proposed structure to minimize the impact of the outliers.
4. Six forecasting models' performances are compared on basis of different subsets of SCADA inputs. The models and generalized stepwise method are depicted in Fig. 1: Preprocessing of data for extraction; Feature extraction; Outliers minimization training and testing; and performance analysis.
5. Finally, because there is no simple theory for designing and tuning a network's hyper-parameters, the model structure and hyper-parameters are updated and fine-tuned by using a novel hybrid optimization combined with Sine Cosine Algorithm (SCA) is fused with a dynamic group based optimization mechanism with two predicting spaces of 10-min and 1-h ahead.

2. Related work

To anticipate the available power in impending events, conventional methodologies depend on physical models combined with numerical weather prediction strategies. These numeric methods are fast but lack efficiency due to highly nonlinear monotonic relationships between the physical indices of operating conditions. To better incorporate parametric relationships, statistical models are being utilized. These methods relate the system inputs to the predicted output for energy forecasting.

The hybrid NN-SI for STWF has been utilized in several scientific studies. Physical models, statistical models, ANN models, and hybrid intelligence approaches are some forecasting methods that anticipate wind power generation [5]. Two methodologies are often integrated

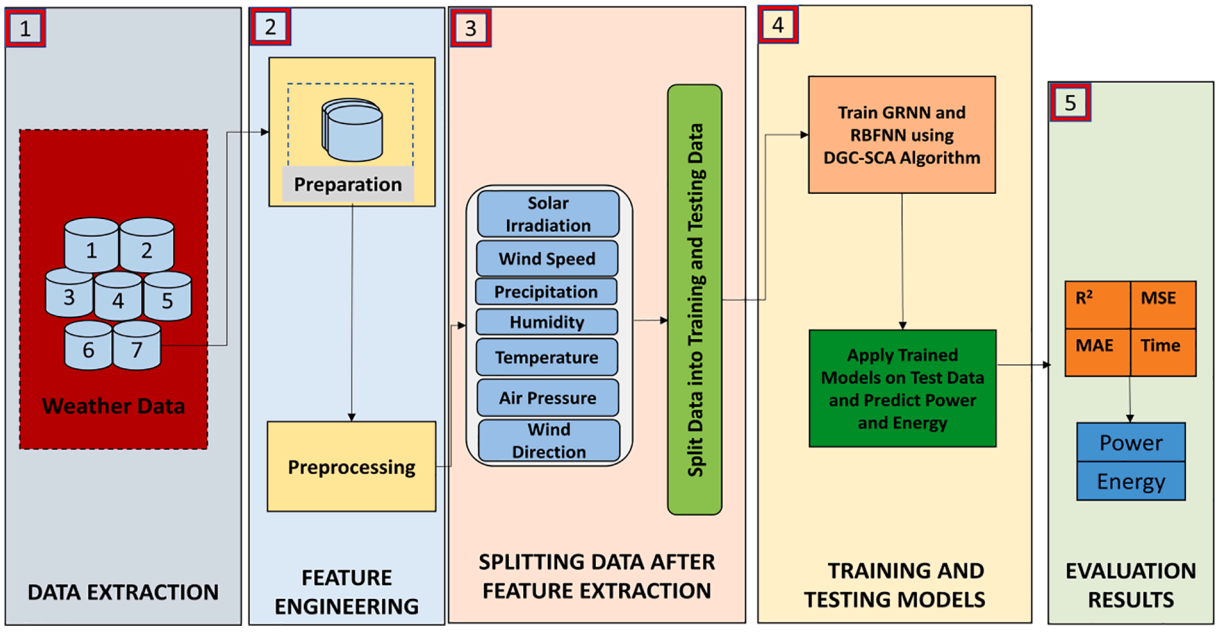

Fig. 1. Graphical presentation of procedure Hybrid PV/Wind Power using IDGC-GRNN and IDGC-RBFN.

into a hybrid intelligent strategy to improve prediction accuracy. It employs fuzzy logic control, machine learning, swarm intelligence, and neural networks. This combination is used to offset the disadvantages of each strategy. The fundamental issue with the fuzzy logic technique is that it necessitates the use of an empirical variable in order to set the explanatory variables [6]. [7] presents a combined SVM and enhanced DFO to estimate wind power generation using adaptive learning parameters and a differential evolution technique. The parameters for SVM are provided by the IDFO. [8] employs a hybrid fuzzy model for interval forecasting of wind speed by multiplexing of the learning Gaussian process. The final Gaussian process model is chosen because fuzzy-driven multiplexers outperform the autoregressive moving average model.

The physical technique, such as numerical weather prediction, utilizes hydro- and thermo-dynamic models of physics and the environment, resulting in poor forecast performance due to the production of precise mathematical models. Statistical approaches, such as probabilistic auto-regression [9] and probability mass bias [10], build mathematical correlations between explanatory variables and generate power. This technique has a problem with flexibility and learning capabilities, and its effectiveness degrades as prediction horizons lengthen. Attention mechanisms and multivariate distribution estimates are required to overcome these challenges. ANN is often used to predict wind power output due to its ability to map nonlinear relationships and adopt self-learning from data samples [11]. The primary benefit of this method is that no mathematical model is required to construct a link between input and output data in order to predict wind power generation [12,13]. [14] develops an NN-based 10-min forecasting method to demonstrate performance by addressing the concerns of over-under fitting in NN. The NN training is prone to data outliers, and a highly random process of learning can generate skewed relationships in trying data and cost functions. The Spatio-temporal framework, the controlled balance between exploration and exploitation processes in swarm intelligence, and effective simultaneous weights and bias improvisation can successfully outperform back propagation (BP) [15]. Typically, SVM struggles with delayed training and poor generalization ability; so, in [16], GWO is used to optimize the SVM technique's kernel function parameter. The most common methods include Kalman filters, time series methods, the persistent method, and machine learning techniques such as KNN, SVM, etc. these moths enhance the prediction efficiency but are susceptible to growing errors over time if the data is not accurate time-stamped, outliers in the data and system model sensitivity. Among time series models the autoregression method (ARM) is better suited for short-term forecasting. These include autoregressive moving average (ARMA), improved using an enhanced integral model in autoregressive integral moving average (ARIMA), and fractional-ARIMA(f-ARIMA).

To overcome the shortfalls of physical models the statistical models show promising results and have been studied thoroughly using different statistical data, mathematical models, and data-driven algorithms [17]. In Yuan et al. [18], the least squares support vector machine (SVM) is adopted for STWF application. The utility of the gravitational search optimization technique is examined to enhance the prediction accuracy further. In many cases, the data is not adequate and may miss few features. A regression model is presented in Akhter et al. [19] to limit this limitation. To undertake uncertainty of prediction, a multiple-Imputations Gaussian process regression is proposed in Liu et al. [20]. The mechanism utilizes expectation–maximization for the estimation mixture components. This technique successfully compensates for the missing data of the data distribution. Hybrid models, such as [21], are used in the literature. The expected shortfalls of hybrid models have increased complexity and less accurate long-term prediction. These models predict wind speed using the wind-power characteristics curve [22]. Most meteorological data is available in time stamps.

In Zhao et al. [23], an extreme learning machine (ELM) is designed for ultra-short wind power forecasting. Reverse time series is utilized for ELM training with a bidirectional mechanism in which ELM and optimization algorithm simultaneously incorporate into the learning process. The assumptions are made to simplify the process, which limits the accuracy and learning rate. A multi-output SVM as an optimization scheme is opted in Zhao and Yongning [24] to use Spatio-temporal (ST) analysis for SVM training. In Wang et al. [25], a new class of NN is employed using singular spectrum analysis. The opposition transition state transition algorithm optimizes this hybrid model. The SVM and Logistic regression limitations are overtaken by modern LSTM [26].

In recent years, the significance of machine learning (ML) techniques is acknowledged due to their ability to deal with uncertain mathematical models and systems. These algorithms have been applied to the wind power prediction problem. The K-nearest neighbors (KNN) using multiple features metrological input data is employed in Yesilbudak et al. [27]. Fast prediction is achieved, however, the accuracy of operation stays significantly lower. In Zameer et al. [28], an SVM establishes a co-relation between wind speed and power utilizing altering the initial individual measurements. The accuracy in the short term is improvised at the expense of accuracy in long-term prediction. A combination of wavelet transform and an SVM is adopted in Liu et al. [29] to balance short- and long-term forecasting. In Devi et al. [30], to obtain an hourly ahead forecasting scheme, the authors utilize swarm intelligence optimization and LSTM for forecasting applications. The hybrid mechanisms show exceptional results as in Wang et al. [31], where a hybrid SVM utilizes the auto-regressive moving average model. Particle swarm optimization (PSO) is embedded in PSO-SVM-ARMA for improved efficiency of prediction. The self-organization and stagnation avoidance of swarms enables the identification of the globally best solution. Similarly, in Zhou et al. [32], the K-means short term memory model (K-Means-LSTM) is presented to handle the time dependencies on time series data. This technique has superior performance for training the network model than the back-propagation (BP) for feedforward neural networks (FFNNs).

The existing hybrid models of supervised learning utilize BP to update the weights and biases of the NN framework. The limitations of BP arise from data outliers and stagnation in training. The explorative capability of IDGC allows for precise attention towards each weight and bias training generating more accurate training patterns.

The rest of this manuscript is organized into 6 subsections. The first section examines current ways of developing power prediction models using analytic and DL techniques. Section 2 elaborates on the structure of the proposed methods and infusion of hybrid HVDM. Section 4 summarizes the characteristics of the SCADA datasets used in this study. The training process for GRNN and RBFN structure, and the experimental methodology. The new outlier identification approach employed in this study is described in Section 4. Section 5 studies observations and analysis for the power prediction results trained by datasets of both raw and clean SCADA datasets. Section 6 provides the concluding remarks.

3. Neural networks for regression

In this section, different neural network models are discussed. GRNN and RBFNN are optimized in this study using a novel proposed technique.

3.1. General regression neural network (GRNN)

This neural network is proposed by SpecNET whose structure is like a monitoring type [33]. The methodology of density function (PDF) using non-parameter technique and by building Bayes decision [34]. The mathematical equation of function is shown in Eq. (1):

$$F_k(x) = \left(\frac{1}{N_K}\right)\left(\frac{1}{2\pi^{n/2}}\right)\left(\frac{1}{\sigma^n}\right)\sum_{j=1}^{Ns} e\left(\frac{-||x - x_{kj}||}{2\sigma^2}\right) \quad (1)$$

where N_K is the samples data points average, n is the input sample number, σ^n is the sample probability width, x is the input Euclidean

distance, and x_{kj} is the weighted average of the observed values. In a classification problem, we assume that the classes are known, so we can neglect the magnitude of absolute probabilistic value and only relative magnitude is needed to be considered. Therefore, Eq. (2) can be re-write as:

$$Y_k(x) = \left(\frac{1}{N_K}\right) \sum_{j=1}^{Ns} e\left(\frac{-||x - x_k||}{2\sigma^2}\right) \tag{2}$$

$$S_w = \sum_{j=1} w_j Y_j \tag{3}$$

In the above equation, σ is the factor of smoothness in these probabilistic neural networks. The prediction accuracy can be more enhanced by the optimal tuning of σ. Inappropriate tuning of σ leads to a large or too few numbers of hidden variables, which causes forever fitting. So, this factor is needed to be trained effectively.

GRNN is a type of probabilistic neural network and it consists of four layers as shown in Fig. 2(a). The first layer is the input layer, which acts as a pass layer for the input. The second layer is the pattern layer, which typically stores the training data and Eq. (2) is implemented, whose output is then passed on to the summation layer, which is the third layer. In this layer, the calculation of Eq. (3) is performed and passed on to the output layer, which then generates the output. The fourth layer is the output layer, which is different from the probabilistic neural network (PNN). In GRNN, this layer is a linear layer and performs the weighted average of the output of the summation layer.

3.2. RBFNN Radial basis function neural network

RBFNN is a simple neural network structure with three layers as shown in Fig. 2(b) that is, the input layer, hidden layer, and the output layer [35]. In order to perform the function approximation or the curve fitting, RBFNN uses the scheme in which members of compactly supported radial basis functions are used. The RBFNN increases the dimension of the feature vector by building up basis function $\varphi(||x - C_i||)$ with Euclidean distance between input and center, which is the difference between typical Machine Learning Algorithm and Radial Basis Function.

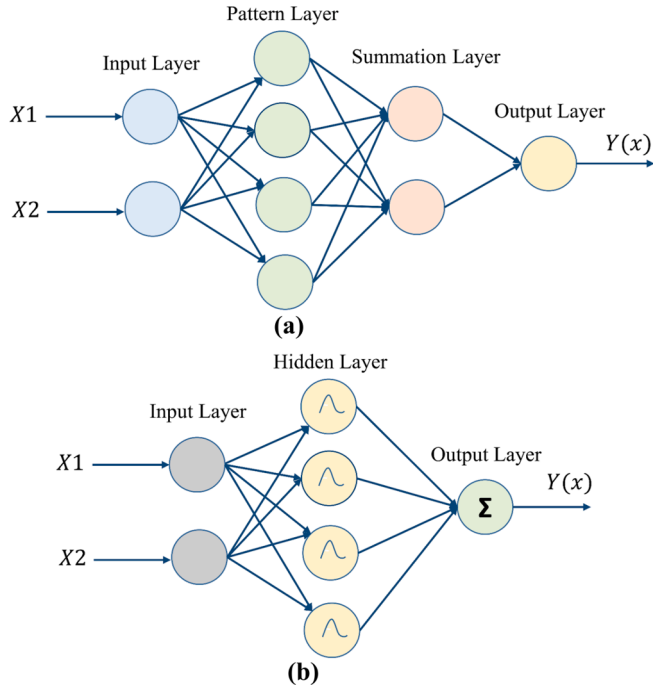

Fig. 2. (a) Four-Layer Structure of General Regression Neural Network; (b) General Structure of Radial Basis Function Neural Network.

The typical radial basis function is:

$$h(x) = e\left(\frac{-(x-c)^2}{r^2}\right) \tag{4}$$

where C is the center, r is the radius and x is the input. In this function with longer distance from the center. So, multi-quadric RBF presented in Eq. (5)-Eq. (6),

$$h(x) = \frac{\sqrt{r^2 + (x-c)^2}}{r} \tag{5}$$

$$f(x) = \sum_{j=1}^{m} w_j h(x) \tag{6}$$

where, w_j are weights connected between the layers in RBFNN.

4. Proposed technique

In this section, a novel *meta*-heuristic optimization algorithm is presented, which is the combination of a dynamic group, based cooperative optimization algorithm and the sine cosine algorithm. This proposed technique combines the merits of both DGCO and SCA. In this technique, the dynamic grouping, property of DGCO is combined with SCA to search around the solution in the exploration phase.

4.1. Dynamic group-based cooperation optimization algorithm

DGCO is a population-based *meta*-heuristic optimization algorithm that uses the exploration and exploited phase for solving complex problems [36]. Unlike other optimization algorithms, DGCO employs a distinct group of particles, namely an exploration group and an exploitation group, both of which operate concurrently. The number of particles in the groups could change if the global best solution is not changing for some iterations. Like all other *meta*-heuristic algorithms DGCO also randomly initializes particles in the search space. Eq. (7) is used to initialize particles:

$$x(i) = m_x + rand() \times (\max\_x - m\_x) \tag{7}$$

where the parcel position is $x(i)$, m_x shows the minimum value of search space and max_x is the maximum value. For randomness $rand()$ is used which generates random particles.

4.1.1. Exploration and exploitation groups: A necessary balance

Since DGCO uses two groups for the updation of particle's position, it is very necessary to maintain a balance of the number of particles in both groups. Initially, the ratio of exploration and exploitation groups is 70%-30%, but over the iterations, the exploration group will decrease and the exploitation group will increase the number of particles to converge towards the global solution. Fig. 3 shows the dynamic grouping of DGCO.

4.1.2. Explorative group

Utility of DGCO with highly explorative behavior in initial phases allows for a better global search which is crucial to maximize search space. In DGCO, the exploration group updates particles position using two methods.

- First it is searching around the current solution for a better solution, whose mathematical modeling is presented in Eq. (8) and Eq. (9).

$$dist = d_1 \times (z(j) - 1) \tag{8}$$

$$z(t+1) = z(j) + dist \times (2d_2 - 1) \tag{9}$$

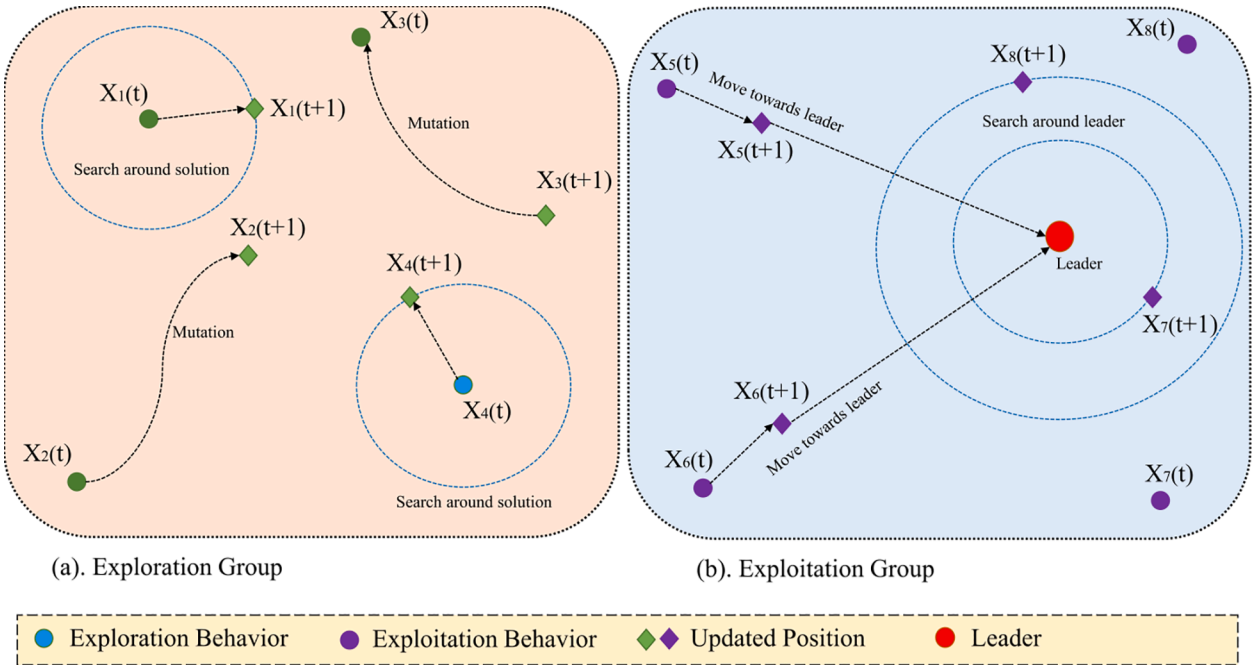

Fig. 3. Dynamic Grouping in Exploration and Exploitation Phases in DGCO.

- The second method uses the mutation to generate and create diversity in the particle position.

4.1.3. Exploitation group

The responsibility of this group is to converge towards a global solution. The exploitation phase defines the best solution finding with good convergence capability. DGCO updates the particles in the exploitation group using two methods.

- First particles search in the ring formed around the particle position for global best using the following equation,

$$dist = d_3 \times (M(j) - z(j)) \tag{10}$$

$$z(t+1) = z(j) + dist \tag{11}$$

where $G(i)$ is the global best solution.

Updating of particles in the second method for exploitation group is searching around the global best solution. This method can be implemented using the following equations.

$$dist = (M(j) \times N - d_4) \tag{12}$$

$$z(t+1) = z(i) + dist \times (2 \bullet d_5 - 1) \tag{13}$$

$$N = 2 - 2 \times \left(\frac{iter^2}{\max\_iter^2} \right) \tag{14}$$

where *iter* are the current iterations and *max_iter* show the max number of iterations. DGCO also uses the concept of elitism in which the global best solution of the previous iteration is transferred to the next iteration also.

4.2. Sine cosine algorithm (SCA)

SCA uses sine and cosine functions to update the particle position by searching around the best solution or the current particle position [37]. In SCA, random initial solutions are generated and the particle position outwards or towards the best possible solution. The structure of the Sine-Cosine Algorithm is shown in Fig. 4.

The mathematical model of the sine–cosine algorithm is presented in the following equations:

$$x(t+1) = X_i + rand() \times \sin(rand()) \times |rand() \times G(i) - x(i)| \tag{15}$$

$$x(t+1) = x(i) + rand() \times \cos(rand()) \times |rand() \times G(i) - x(i)| \tag{16}$$

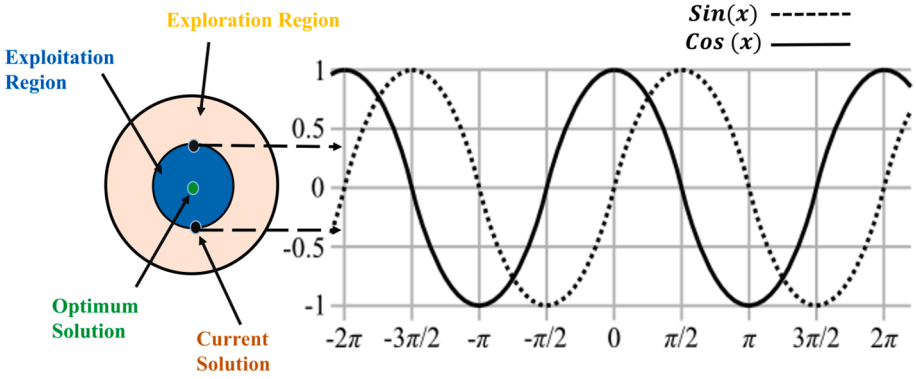

Fig. 4. Structure of Sine-Cosine Algorithm for updation of Particle Position.

The updating of particle position is dependent upon $rand()_1$ as presented in Eq. (17).

$$x(t+1) = \begin{cases} X_i + rand() \times \sin(rand()) \times |rand() \times G(i) - x(i)| & rand()_1 < 0.5 \\ X_i + rand() \times \cos(rand()) \times |rand() \times G(i) - x(i)| & rand()_1 > 0.5 \end{cases} \quad (17)$$

4.3. Dynamic group-based cooperative algorithm with sine cosine algorithm (IDGC)

Since DGCO and SCA are able to perform with greater efficiencies under different optimization problems. However, under complex optimization problems, these algorithms do not perform well due to trapping in the local minima. To overcome this issue, a new strategy is developed for the updating of particle position in the explorative group in DGCO, SCA is used to update the particle position in the explorative group.

In the explorative group of DGCO, the first method uses d to search around the particle position. This updating of d is done by SCA in this proposed technique. In addition, the mutation factor for the second method is also not very effective. In this second method, particle position is also updated using SCA. High efficiency, high convergence speed are the improvements observed in the proposed technique. The integration of SCA in DGCO is presented in mathematical form in the following equations.

In the first method, the updation of the particle is happening in the following way.

$$di = \begin{cases} rand() \times \sin(rand()) \times |rand() \times M(j) - z(j)| & rand()_1 > 0.5 \\ rand() \times \cos(rand()) \times |rand() \times M(j) - z(j)| & rand()_1 \le 0.5 \end{cases} \quad (18)$$

$$X(i+1) = X(i) + 2 \times d \quad (19)$$

In the second method, the following model utilized:

$$di = \begin{cases} rand() \times \sin(rand()) \times |rand() \times M(i) - z(j)| & rand()_1 > 0.5 \\ rand() \times \cos(rand()) \times |rand() \times M(i) - z(j)| & rand()_1 \le 0.5 \end{cases} \quad (20)$$

$$N(j+1) = N(j) + (2 \times rand() - 1) \times di \quad (21)$$

The pseudo-code and flow-chart of the proposed IDGC are shown in Fig. 5 and Fig. 6 respectively.

4.4. Comparative analysis of IDGC

In this section, comparative analysis presented of IDGC with another *meta*-heuristic optimization algorithm. The hardware used for the testing of the algorithm is AMD PRO A8-9800 Rs with 8-GB RAM and the

Initialize *Algorithm parameters (size of population, iteration count)*
initialize *population* $X=X_1, X_2, X_3, \ldots, X_n$
while$(t<iter\_max)$
evaluate fitness of every energy particle, select the best solution
$K=2-2\times {}^{t}/_{iter\_max}$
update particles number's in every group
if *the global best solution doesn't alter from the prior 2 iterations*
increase the particles number's in exploration group
end if
for *every solution in the exploration group*
update the value of r_1, r_2 *and P*
find global best solution by applying elitism
if $P \ge 0.5$
Update Particle Position using Eq. (18)-Eq.(19)
else
Update Particle Position using Eq. (20)-Eq.(21)
end if
end for
for *every solution in exploitation group*
find global best solution by applying elitism
update the value r_2, r_3, r_4, *and P*
if $P \ge 0.5$
update positon in direction of best solution using Eq. (10) and Eq. (11)
else
keep searching around best solution using Eq. (12) – Eq. (14)
end if
end for
update solution that goes beyond the limit.
update prev_fitness_1, prev_fitness_2
end while
Return *Global Best Solution*

Fig. 5. Pseudo Code of Proposed IDGC Algorithm.

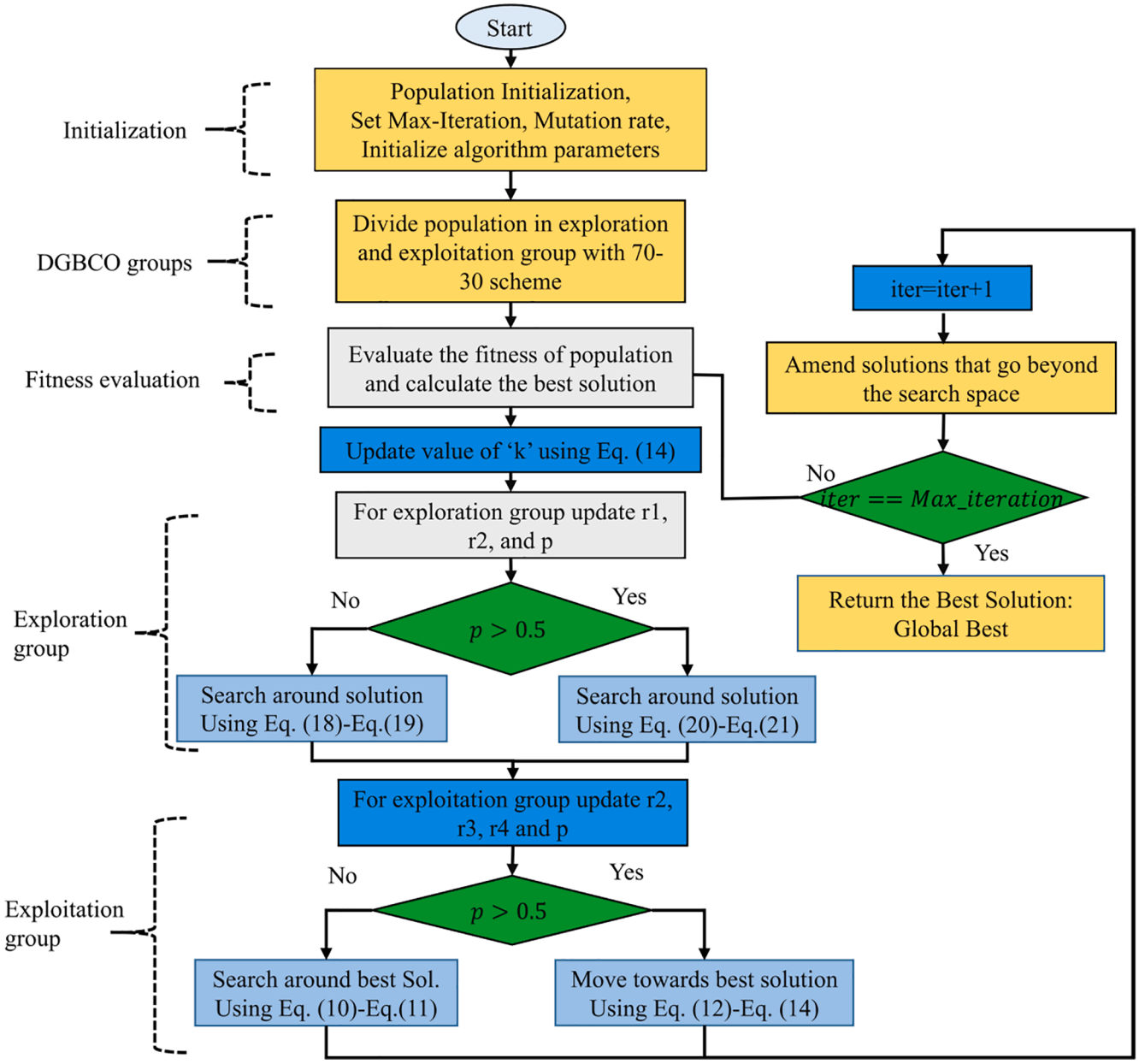

Fig. 6. Flow Chart of Proposed IDGC Algorithm for Particle Position update.

software used is MATLAB 2018a.

The proposed algorithm is tested on 6 different unimodal and multimode test functions. These functions with upper and lower bound are presented in Table 1. The comparison is made between PSO, GWO, FPA, BMO, DGBCO, and IDGC. The convergence curves for all six functions are shown in Fig. 7 which shows that the IDGC algorithm achieves better results by minimizing the function in a fewer number of iterations and the cost achieved by IDGC is far less than other techniques. The performance of all techniques can also be compared by the values achieved in Table 2. The performance indices are the best value, worst value, average, and standard deviation. It is also confirmed that IDGC outperforms other techniques.

Table 1
Uni-modal and Multimodal Functions with dimensions used for Testing of IDGC.

Func.	Formulae	Dimension	Range	Optimal Value
F1	$f(x) = \sum_{i=0}^{n} \lvert x_i \rvert + \prod_{i=0}^{n} \lvert x_i \rvert$	30	[-10,10][13]	0
F2	$f(x) = max_i\{\lvert x_i \rvert, 1 \le i \le n\}$	30	[-100, 100]	0
F3	$f(x) = \sum_{i=1}^{n} x_i^2$	30	[-100,100]	0
F4	$f(x) = \sum_{i=1}^{n} [x_i^2 - 10\cos(2\pi x_i) + 10]$	30	[-5.12,5.12]	0
F5	$f(x) = -20e^{\left(-0.2\sqrt{\frac{1}{n}\sum_{i=1}^{n} x_i^2}\right)} - e^{\left(\frac{1}{n}\sum_{i=1}^{n}\cos(2\pi x_i)\right)} + 20 + e$	30	[–32,32]	0
F6	$f(x) = 1 + \frac{1}{4000}\sum_{i=1}^{n} x_i^2 - \prod_{i=1}^{n}\cos\left(\frac{x_i}{\sqrt{i}}\right)$	30	[-600,600]	0

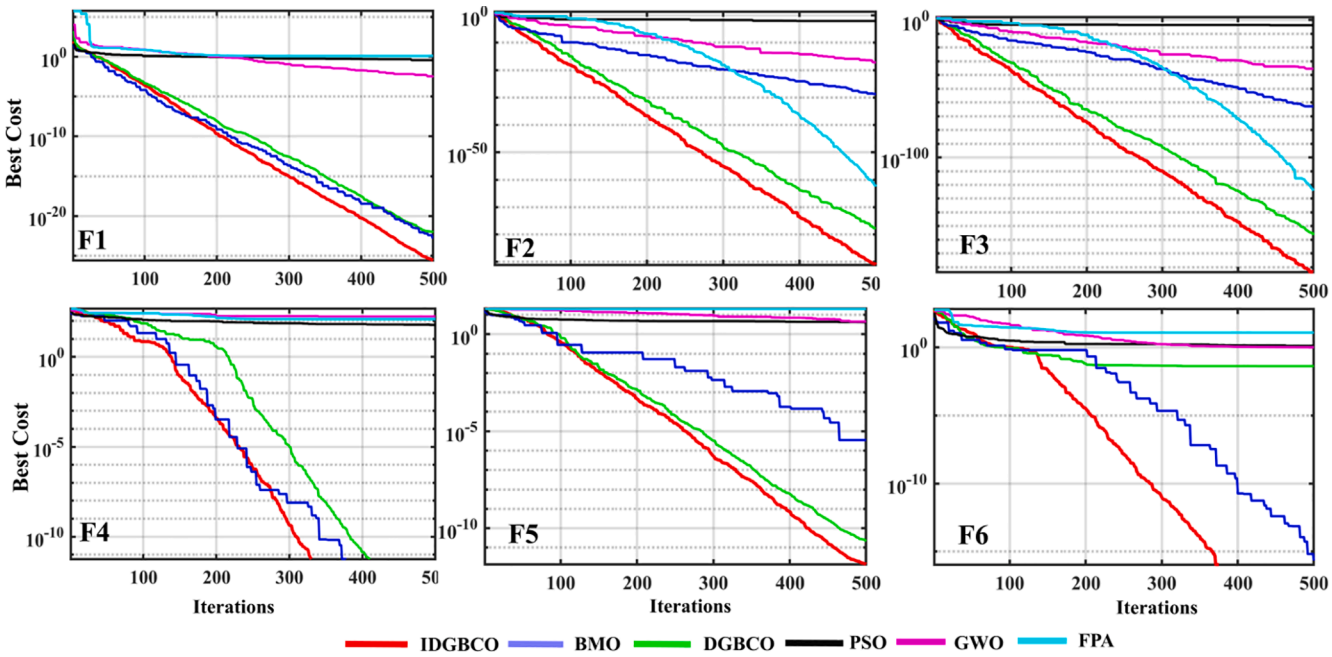

Fig. 7. Convergence curves comparison of test functions for comparative techniques.

Table 2
Comparison results for IDGC, DGCO, BMO, DFA, FPA and PSO optimization technique on test functions.

Functions	Parameters	PSO	FPA	DFA	BMO	DGCO	IDGC
F1	Best	1.0654e+00	1.0919e+00	6.1906e-01	1.1866e+00	7.5599e-01	7.6067e-01
	Worst	3.3183e+00	2.8628e+00	3.8153e+00	4.3919e+00	3.5328e+00	2.6240e+00
	Avg	1.8393e+00	1.7735e+00	1.7069e+00	1.8424e+00	1.8961e+00	1.5810e+00
	Std	5.1143e-01	4.3011e-01	5.6395e-01	5.7943e-01	6.4277e-01	3.7090e-01
F2	Best	6.6922e-03	3.3945e-03	4.7698e-03	6.0814e-03	1.6544e-02	1.5854e-03
	Worst	1.1381e-01	1.0411e-01	1.1132e-01	8.9605e-02	9.9858e-02	7.7334e-02
	Avg	4.5564e-02	3.7035e-02	3.6736e-02	3.8232e-02	4.0218e-02	3.7157e-02
	Std	3.1212e-02	2.7009e-02	2.3888e-02	1.9897e-02	1.9219e-02	1.9773e-02
F3	Best	2.2654e-06	6.3339e-05	5.3836e-05	1.4876e-04	1.3072e-05	6.9877e-06
	Worst	1.2967e-02	1.9226e-02	9.5308e-03	1.9549e-02	1.1735e-02	1.1762e-02
	Avg	3.7238e-03	2.4777e-03	2.2740e-03	4.1696e-03	2.9321e-03	2.1681e-03
	Std	3.6706e-03	3.8117e-03	2.4986e-03	5.2296e-03	3.5136e-03	2.9309e-03
F4	Best	7.9726e+01	7.6398e+01	9.3708e+01	8.4380e+01	1.0531e+02	7.3486e+01
	Worst	1.6835e+02	2.0112e+02	1.8169e+02	1.9579e+02	1.7586e+02	1.8030e+02
	Avg	1.2952e+02	1.2955e+02	1.3894e+02	1.2898e+02	1.3130e+02	1.2830e+02
	Std	2.1996e+01	2.4777e+01	2.0990e+01	2.3905e+01	2.1360e+01	2.0057e+01
F5	Best	4.7144e+00	3.7397e+00	4.2750e+00	4.2796e+00	4.4399e+00	3.8889e+00
	Worst	6.9701e+00	6.5207e+00	6.4176e+00	6.8326e+00	6.2143e+00	6.1367e+00
	Avg	5.5445e+00	5.2546e+00	5.3881e+00	5.3322e+00	5.2514e+00	5.2592e+00
	Std	5.3648e-01	6.0239e-01	5.2854e-01	5.4322e-01	4.7795e-01	5.2141e-01
F6	Best	2.4183e+00	2.0644e+00	2.1353e+00	2.2210e+00	2.0899e+00	1.7703e+00
	Worst	5.7100e+00	4.5009e+00	4.5312e+00	4.3186e+00	4.2298e+00	4.2056e+00
	Avg	3.1342e+00	3.0003e+00	3.0786e+00	3.0543e+00	3.1071e+00	3.0092e+00
	Std	6.8570e-01	5.5604e-01	5.5880e-01	5.0741e-01	4.9782e-01	3.3881e-01

4.5. Training of GRNN and RBFNN using IDGC

GRNN and RBFNN suffer from low prediction accuracy if the parameters, e.g., σ smoothing parameter with the number of neurons in RBFNN do not tune well. For effective training and testing these parameters are needed to be optimally tuned. In this paper, IDGC is used to tune these parameters, and hybrid PV/wind power and energy forecasting are done. The flow chart for the training of GRNN and RBFNN using IDGC is shown in Fig. 8. Trained models are then tested on the test data and the performance evaluation is done.

5. Experimental test results

In this section, IDGC-GRNN and IDGC-RBFN prediction models are

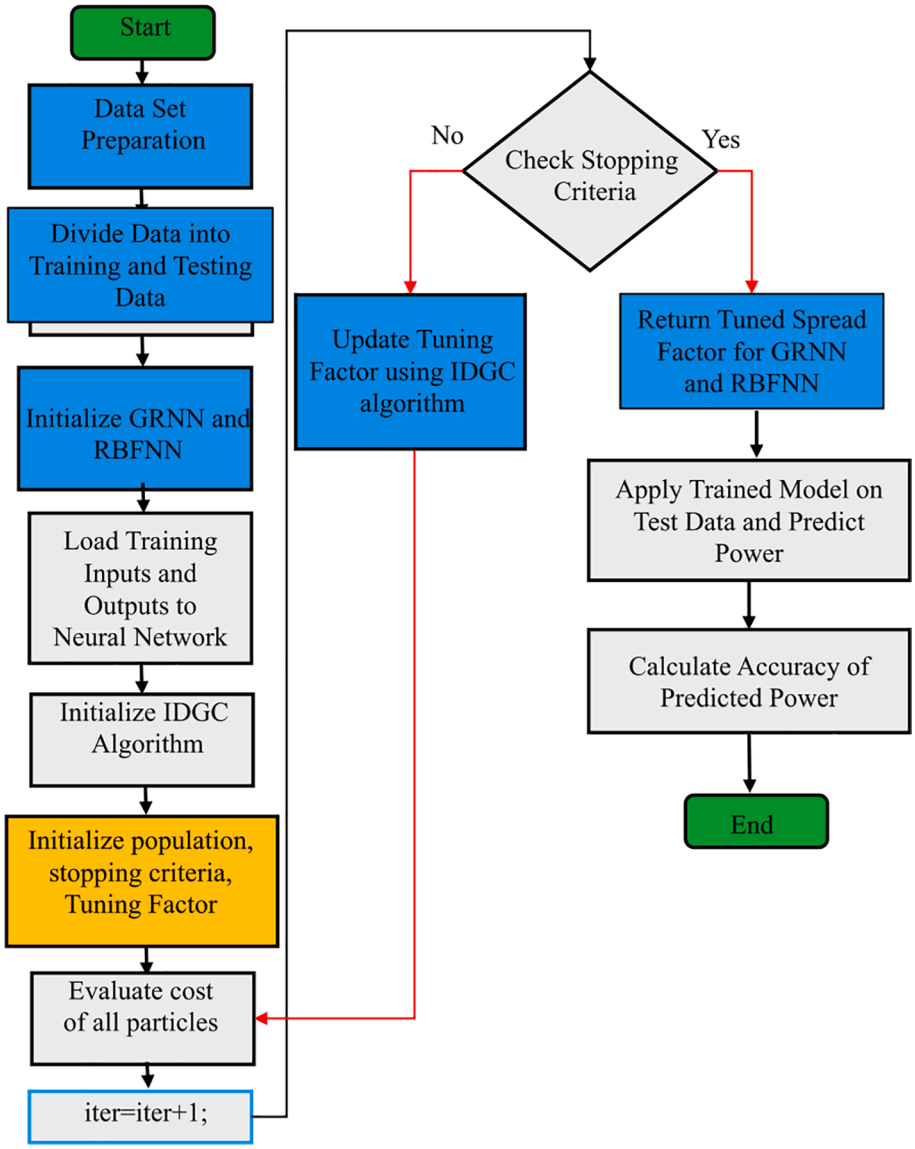

Fig. 8. Flow Chart for Optimal Tuning of GRNN and RBFNN using IDGC.

presented. First data collection and preparation are described. Then the objective function is explained. Successively, the evaluation indices, which are used for the performance comparison, are considered. Then the predictions model and results are discussed for hybrid PV/wind power.

5.1. Data collection and processing

Historical dataset with 1 h sample time was gathered using calibrated sensors which are placed in middle east technical university (METU) from 01/01/2015 till 26/12/2015. For the hybrid power plant, all the environmental factors affect the performance of the power plant. Therefore, seven different factors are then accounted for effective reduction of power. These factors are wind, speed (w_s), wind direction (w_d), solar irradiance (G), temperature (T), the pressure of atmosphere (P), precipitation (R), and humidity (H). The global positioning system (GPS) module of raspberry pi was used for the collection and gathering of the data. After the collection of data, two important functions are applied to the data:

- Feature engineering;
- Normalization.

First, the dataset is analyzed and a feature section is done. All the features that are having an impact on the PV/wind power and energy are selected. Only 7 environmental factors are selected as features remain in the dataset. After that, data normalization is carried out. Since, the large fluctuation in the features, that is, wind, speed, or direction could cause the accuracy of the prediction model to become low. Therefore, the applied normalization technique is applied, which is shown in Eq. (22).

$$X_{norm} = \frac{X_i - X_{min}}{X_{max-X_{min}}} \tag{22}$$

where X_{norm} is the normalized values and X_i the current value, X_{min} and X_{max} are minimum and the maximum values of the data.

Table 3 shows the descriptive statistics of the dataset. Five parameters are used for the analysis, that is, count, max value, min value, standard deviation, and mean. For all four seasons, the samples are 8632. This shows the real-time diversity in the dataset which is catered by IDGC-GRNN and IDGC-RBFNN very effectively during the training and testing. Then with the help of timestamp, this dataset is then further divided for all four seasons and predicted models are trained and tested on all four seasons. For every season the training to the testing ratio of the dataset is 3:1. Mean variation in the values of features in the dataset

Table 3
Descriptive Statistics of the Dataset.

Indices	Wind Speed	Temp.	Humidity	Air Pressure	Wind Direction	Precipitation	Irradiance	Power	Energy
Count	8632.00	8632.000000	8632.000000	8632.000000	8632.000000	8632.000000	8632.000000	8632.000000	8632.000000
Mean	0.40785	0.186580	0.709743	0.996968	0.182660	0.254109	0.207660	0.679220	0.611298
Std	0.22987	0.074352	0.152935	0.005119	0.077407	0.101936	0.284296	0.067437	0.060694
Min	0.04000	−0.010000	0.130000	0.830000	0.000000	0.090000	0.000000	0.514000	0.462600
Max	1.00000	1.000000	1.000000	1.000000	0.360000	0.560000	1.000000	0.910200	0.819200

shows how the parameters/factors are varying. The mean variation in temperature is 0.18, wind 0.4, pressure 0.99, humidity 0.7, irradiance 0.2. Minimum and maximum values of features are given in Table 3.

5.2. Objective function and evaluation parameters

A fitness function or objective function is used for the training and testing of models. The lower values of the fitness function show that the data predicted by the model is close to the true values. Therefore, the fitness function defines the prediction accuracy. The most widely used fitness function is the mean square error (MSE) which is presented in Eq. (23).

$$F.F = \frac{1}{n}\sum_{i=1}^{n}(T_i - P_i) \tag{23}$$

where T_i is the true value and P_i are the predicted value and n represent the total number of samples. For the evaluation of different models, other error indices are also used. The degree of dispersion in results can be verified by normalized root mean square error (NRMSE) presented in Eq. (24). For the indication of deviation of prediction mean absolute error (MAE) and mean absolute percentage error (MAPE) is presented in Eq. (25) and Eq. (26) respectively. Last but not the least, the correlation between actual and predicted value can be measured by R square (R^2) which is presented in Eq. (27).

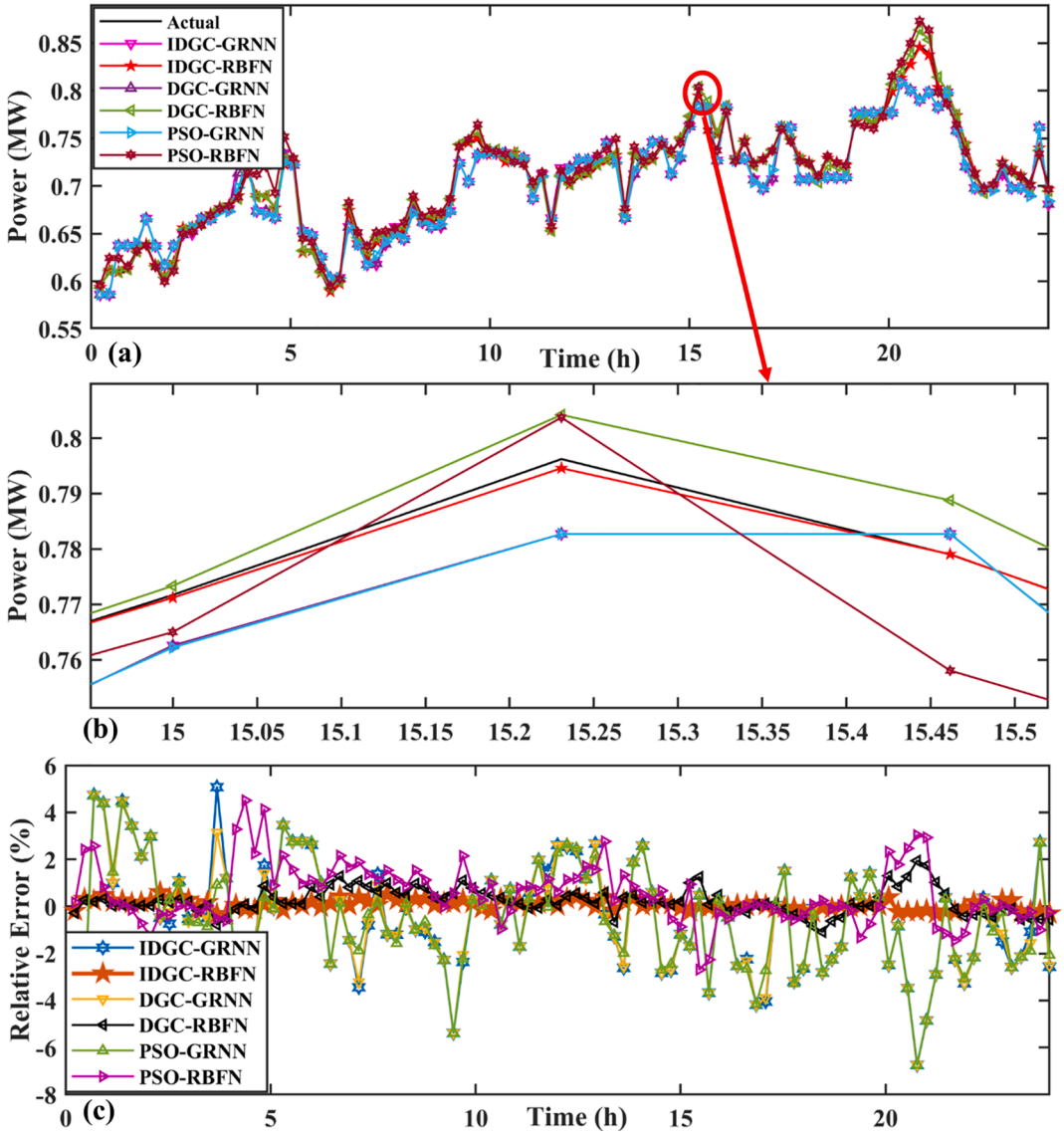

Fig. 9. (a) Prediction in summer season (b) Zoomed-in Comparison Summer season (c) Percentage Relative Error for Summer Season.

$$NRMSE = \frac{1}{T}\sqrt{\frac{1}{N}\sum_{i=1}^{N}(T_i - P_i)^2} \times 100\% \quad (24)$$

$$MAPE = \frac{1}{N}\sum_{i=1}^{N}\frac{|T_i - P_i|}{P_i} \times 100\% \quad (25)$$

$$NMAE = \frac{1}{N}\sum_{i=1}^{N}\frac{|T_i - P_i|}{P_i} \quad (26)$$

$$R^2 = \frac{\sum_{i=1}^{N}(T_i - \overline{T_i}))\bullet(P_i - \overline{P_i})^2}{\sum_{i=1}^{N}(T_i - \overline{T_i})\bullet\sum_{i=1}^{N}(P_i - \overline{P_i})} \quad (27)$$

where T_i is the true value, P_i is the predicted value, N is the total number of samples. $\overline{T_i}$ is the average value of the true output, $\overline{P_i}$ is the average value of predicted output.

5.3. Proposed IDGC-GRNN and IDGC-RBFN prediction models

The procedures of prediction of hybrid PV/wind power are shown in Fig. 9. First, collected data is preprocessed to extract features. Seven features are extracted. The data is divided into training and testing data for four seasons. Then training of GRNN and RBFN based NN is done using the IDGC algorithm. Finally, the trained model is evaluated using test data. A set of comprehensive evaluation indices is utilized to evaluate the prediction results using Eq. (24)-Eq. (27).

5.4. Experimental results and discussion

In this section, the prediction results of different models are discussed. Six different models are compared which IDC-GRNN, IDGC-RBFN, DGCO-GRNN, DGCO-RBFN, PSO-GRNN, and PSO-RBFN. The tuned parameters achieved by all the models are presented in Table 4.

5.4.1. Forecasting module

After the original SCADA data has been preprocessed and the proposed IDGC algorithm has been initialized, the training samples are separated based on the weather. The sub-series are fed into the trained SI-NN model, which predicts future changes with great accuracy. Each sub-series of testing data has distinct features, and stability is extensively investigated. The superiority of the designed data preparation module and optimization method determines performance. As a result, in engineering applications, it can offer the desired predicting outcome.

5.4.2. Summer season

The Vector map in Fig. 9(a) shows that the summer season in Turkey has larger variations in wind torrents due to strong winds. The difference between day and night temperatures is high (Avg. Summer 23 °C, Avg. Winter −2 °C). The performance of the proposed technique is also compared for the summer season. Fig. 9(a) shows a comparison of power achieved w.r.t. time by competing techniques and corresponding detailed power prediction is presented in Fig. 9(b). The power in the summer season is highly non-linear but still proposed algorithm achieves efficient prediction for the actual value for GRNN and RBFN models. The performance of proposed techniques in the summer season can also be validated by the relative error shown in Fig. 9(c) where the least RE depicts higher efficiency of prediction.

A comparison is made with true wind power and predicted wind power by all four techniques. The data is divided into training and testing by ratio of 67% and 33% respectively. Firstly, all techniques are trained on a training dataset with optimally tuned parameters. Then proposed method and other comparative techniques are tested on the testing dataset. Table. 5 shows the minimum error achieved by all techniques during the training and testing process which shows that the suggested strategy achieves less inaccuracy than the other strategies. The training accuracies for the winter season show on run average 0.08 RE which shows that the IDGB based NN effectively minimizes cost function in fewer epochs comparatively. The power predicted by the IDGC-GRNN and IDGC-RBFN is close to the measured data. This shows that prediction is highly effective for the prediction of the highly volatile wind power dataset.

5.4.3. Spring season

The volatility of atmospheric parameters in different seasons in the Sea of Marmara has a transitional effect on Oceanic and Mediterranean climates. Moderately dry summer (≅ 30°C) with high precipitation in Spring yield less fluctuation and the coast prevents elongated winter. Hence, more accurate prediction is expected. The PSO algorithm, due to its highly random behavior, shows the largest error since the cross-correlation between the operating conditions is not accurately translated into the training of the RBFN and GRNN [38]. The proposed methods achieve 70% less RE. The combination of PSO-RBFN shows the least accurate metrics. PSO vigorously manipulates the shorter volatile learning process of RBFN as a BP alternative although trains the system but is highly prone to data outliers. On average, the framework has 67%

Table 4
Optimal Tuned parameter for the GRNN and RBFNN using Optimization Techniques.

	PSO		DGCO		IDGC	
	Spread	Neurons	Spread	Neurons	Spread	Neurons
GRNN	0.021	X	0.012	X	0.009	X
RBFNN	39	196	56	204	61	208

Table 5
Statistical comparison Results summary for different seasons.

Season	Technique	RMSE	MAE	R^2	Mean RE
Summer	IDGC-RBFN	**7.3398e-05**	**2.2242e-08**	**0.1161**	**0.0327**
	IDGC-GRNN	3.0225e-04	9.1590e-08	0.2125	0.9927
	DGC-RBFN	2.3272e-05	2.3272e-06	0.1397	0.3645
	DGC-GRNN	3.8333e-04	1.1616e-07	0.2295	1.0003
	PSO-RBFN	1.1925e-04	1.1925e-05	0.1616	3.6466
	PSO-GRNN	6.5592e-04	6.5592e-05	0.2890	0.9854
Spring	IDGC-RBFN	**7.9896e-05**	**7.9896e-06**	**3.5831e-04**	**0.0241**
	IDGC-GRNN	4.1369e-04	1.0210e-04	4.1644e-04	0.1114
	DGC-RBFN	5.3789e-04	5.3789e-05	5.1132e-04	0.3468
	DGC-GRNN	0.00091	1.9320e-04	5.2616e-04	0.1090
	PSO-RBFN	5.1076e-04	5.1076e-05	6.1768e-04	0.6082
	PSO-GRNN	0.0018	1.8000e-04	4.1651e-04	0.1063
Winter	IDGC-RBFN	**1.0853e-04**	**1.0612e-05**	**0.9154**	**0.0847**
	IDGC-GRNN	8.5311e-04	8.3654e-05	0.9894	0.4128
	DGC-RBFN	1.6350e-04	1.6032e-05	0.9300	0.2672
	DGC-GRNN	8.5311e-04	8.3654e-05	0.9982	0.4321
	PSO-RBFN	9.7869e-04	9.5969e-04	0.9951	0.5807
	PSO-GRNN	8.5311e-04	8.3654e-05	0.9987	0.4583

more error margins. Fig. 10(a) shows that during daytime (0–24 Hours) the algorithms using higher random factors tend to generate higher error margins leading to lower power tracking efficiency. This duration falls typically in the "Peak Hours" where the energy demand surge occurs, making it a daunting task to predict the power generation in a shorter time accurately. A more detailed view of results in spring season is presented in Fig. 10(b). The percentage Relative Error in Spring Season is shown in Fig. 10(c).

5.4.4. Winter season

The winter data shows relatively higher training and testing accuracies. It may owe to lower fluctuation of data. PSO-based SI-NN has the least accuracy for both GRNN and RBFN. IDGB shows 81.92% less RMSE values as compared to DGC on average. Whereas the PSO shows huge errors in predictions. This failure to predict the actual power can cause voltage fluctuations leading to a harmonic imbalance in grid-connected power generation systems. It may lead to a pole-pole fault in high voltage grids. Comparatively, the error margin of the proposed forecasting model allows for the negligible error margins that can be easily handled by the grid monitoring systems and HVDC protection mechanism well within 0.3 s [39]. Fig. 11(a) shows the forecasting performance on a standard 24 h winter days. Fig. 11(b) provides a detailed comparison in a smaller window of time whereas Fig. 11(c) provides the %age RE with respect to the actual power for competing techniques.

6. Common observation

Three criteria were used to assess the performance of proposed technique for extremely short-term prediction: MAE, RMSE, and the MAPE. For each analysis, 20 runs are performed to provide a fair comparison. The following is a quick description of these indexes.

Normalized Root Mean Square Error (NRMSE): The NRMSE is the standard deviation of a sample's prediction errors. It represents the distribution of errors, with a larger value suggesting a higher spread of errors. Because a larger difference between actual and predicted values has a greater value on NRMSE than NMSE, the value of NRMSE is often higher than NMSE due to the presence of outliers, as demonstrated by Eq. (24).

Mean Absolute Percentage Error (MAPE): which is the percentage counterpart of NMAE, quantifies how far the model's predicted values are off from their actual values on average. Since this approach also employs absolute value, it is immune to the impact of outliers such as NMAE. This approach is beneficial for interpreting model performance as NMAE and NRMSE to present a value ranging from zero to positive

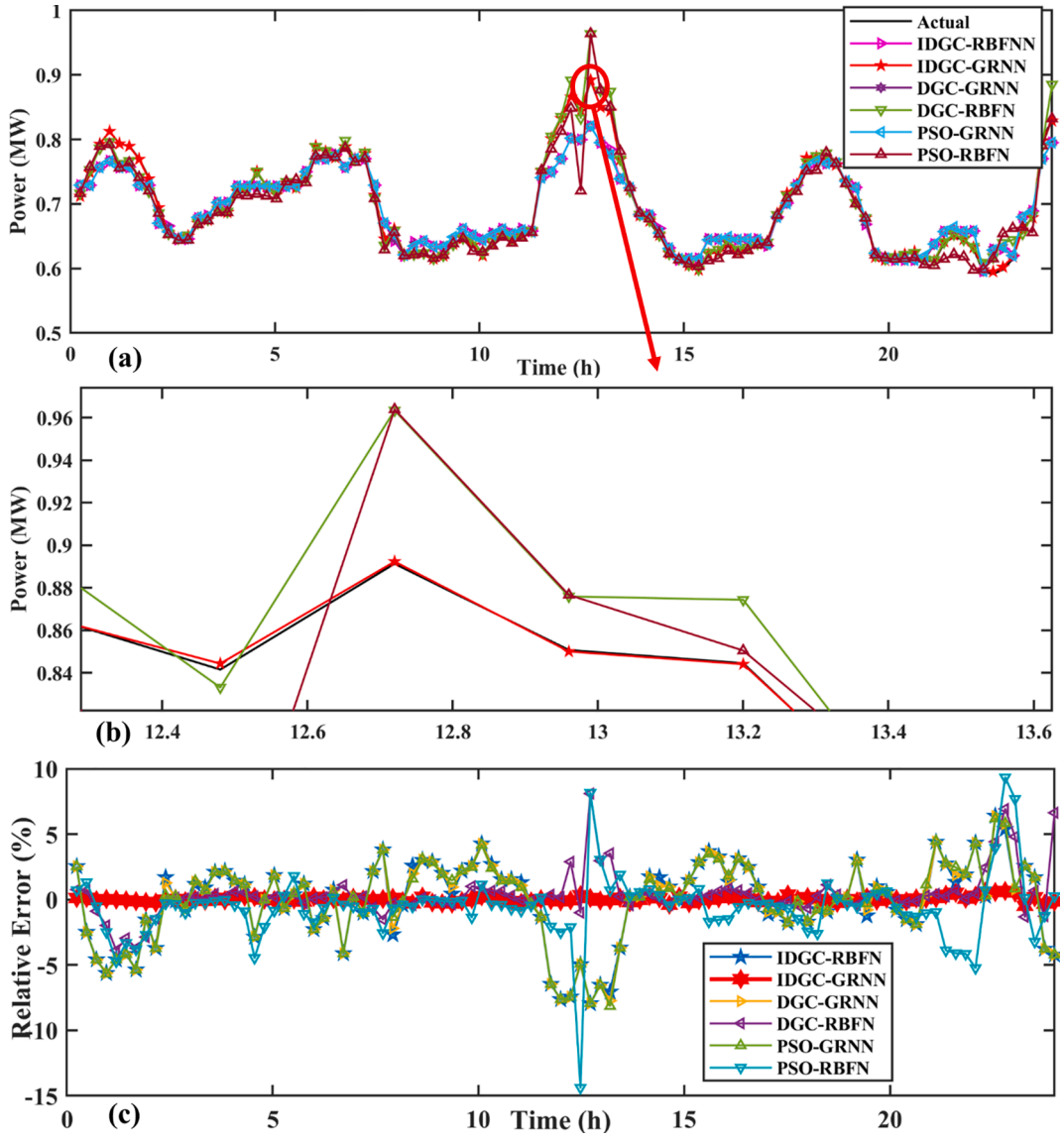

Fig. 10. (a) Prediction in Spring season (b) Zoomed-in Comparison Spring season (c) Percentage Relative Error in Spring Season.

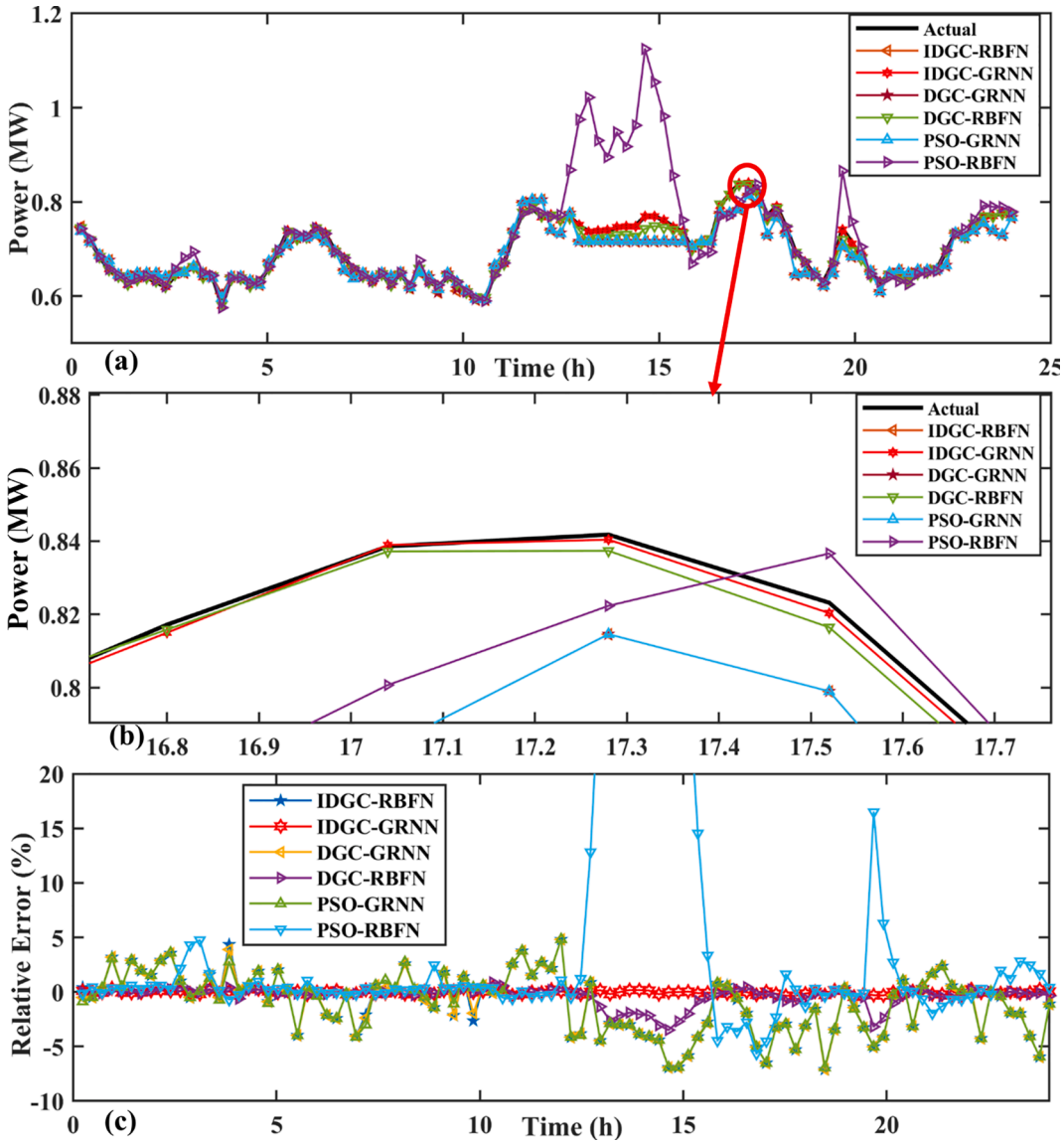

Fig. 11. (a) Prediction of power in Winter season (b) Zoomed-in Comparison Winter season (c) Percentage Relative Error for Winter season.

infinity using percentages, i.e., forecasted values are scaled against the real value. As a result, when the real data is 0 or extremely small, it may calculate an unexpected number. Eq. (25) provides the formula for calculating NMAPE.

The NMAE (Normalized Mean Absolute Error) is the average magnitude of absolute errors between actual and predicted values. It takes absolute values into account to avoid cancellation between negative and positive error values and hence does not refer to the model's underperformance or overperformance. The NMAE is a useful performance statistic for mitigating the effects of data outliers or extreme values in data sets. A low NMAE value denotes great prediction accuracy, but a zero NMAE value denotes the most accurate model for predicting output data. Eq. (26) represents its mathematical.

The lower the MAE and RMSE, R^2 and MAPE values, the better is forecasting performance. All the models are tested on four different seasons, that is, winter, summer, autumn, and spring. The average value of the evaluation index is shown in Table. 5. This shows that IDGC-RBFN outperforms other techniques. The IDGC-RBF achieves up to 80% less NRMSE, 6.4978×10^{-5} less NMAE, up to 90% less MAPE, and 0.1729–0.582 less R^2 as compared to together DGC-RBFN and DGC-GRNN. This shows that the proposed technique has higher prediction accuracy. This 24 h prediction comparison shows that IDGC-RBFN performs with higher accuracy for the short-term power prediction.

6.1. Forecasting stability

The proposed techniques show high stability and forecasting. The measure for performance variance of forecasting error in [40] is well suited to determine the stability of prediction. The smallest magnitude of absolute error and low variability indices indicate a higher %age accuracy. The forecasting by developed methods shows the least outlier influence and shows precise prediction well within the range of 2–5% of the average of the competing methods.

6.2. Practical application of forecasting model

The forecasting model finds are utilized for the following applications and objectives [38].

1. The accurate forecasting of hybrid PV-wind adds to the competitiveness of renewable energy in the utility market. It solidifies the foundation of renewable power making it capable to compete for price, intermittence, market share and reduces the uncertainty of operation.

2. Improved power grid scheduling impacts the usage of fossil fuels and reduces the CO_2, SO_2 and fog in the environment while providing highly effective real-time load balancing. It lowers the risk of adverse effects of grid-connected operations by commercial-scale PV-Wind further reduces uncontrollability issues of wind power.
3. Safe operations of the power grid are ensured by improvised forecasting. Most power grids are AC, the voltage fluctuations impact the harmonic balance in load-lines. The proposed models with effective forecasting time allow for the rotating reserve capacity minimizing the cost of operations

6.3. Training real time assessment

To assess the computational cost of the hybrid model, GRNN and RBFN training are carried out as the backbone of the suggested model for a variety of learning rates, batch sizes, and iteration numbers. Fig. 12 shows the GRNN and RBFN runtime landscape several parameters. It has been discovered that batch size, learning rates, and data are major factors in the computational cost of training. As per these observations, the larger number of iteration cycles for IDGC with a small batch size of training data having an NN learning rate between 0.012 and 0.09 better achieve effective power forecasting results.

6.4. Computational complexity

The computational complexity of the recommended hybrid frameworks is examined by comparing the mean duration of several iterations for hybrid models. It is worth mentioning that evolutionary algorithms have the same population size. The computing time necessary to apply evolutionary operators such as initialization, fitness function evaluation, hyper-parameter optimization, and finally cost function evaluation. In terms of runtime, using the parallel training configuration yields the best results. This concurrent training setup can significantly reduce computational runtime. The proposed NN may be taught utilizing soft platforms, and the trained NN configuration is then exported into microcontrollers. However, there are certain computing overheads, mostly due to data transfers, synchronization, thread creation, and removal.

7. Conclusion

Modern power grids are a combination of volatile renewable and environmentally hazardous fossil fuel-based electrical power generation systems. To strike a balance between maximum green energy production and stably safe grid operations, the power forecasting of renewable systems is an essential component. Due to meteorological factors, irradiance, precipitation, humidity, etc., the available power fluctuates. Additionally, the time-series data from operating microgrid exhibit chaotic behaviors making the forecasting unreliable. In this work, a combination of outlier detection and feature selection to decrease the inherent noise in time series meteorological data. In the second phase, a hybrid SC-Algorithm (SCA) and DGB optimization are developed to minimize the NN training for hyper parameters. The performance of the improvised IDGB model is tested on modern test functions. The hybrid NN– meta heuristics optimization method is utilized to effectively design IDGBO-GRNN and IDGB-RBFN. Extensive simulated experiments are conducted for seasonal performance evaluation in Summer, Autumn, Winter, and Spring. The average efficiency is significantly higher. The suggested technique is compared with four different hybrid models. As per the results, the suggested hybrid model beats its counterparts in terms of four statistical criteria in both 10-min and 1-h periods.

In the future, a broader range of power curve datasets obtained from other types of wind turbines in other areas will be reviewed in order to improve our model even more. Finally, another exploration of this project is to use various outlier identification methodologies with decomposition and optimization to enhance predicting outcomes.

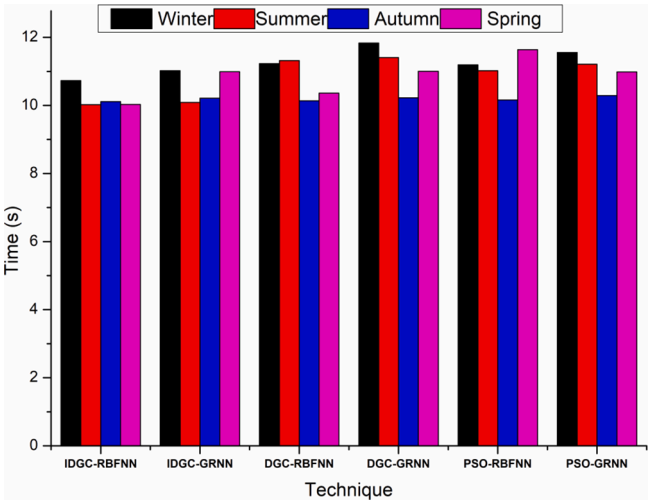

Fig. 12. Runtime Parameters of different techniques.

CRediT authorship contribution statement

Muhammad Hamza Zafar: Conceptualization, Methodology, Resources, Project administration. **Noman Mujeeb Khan:** Validation, Data curation, Software. **Majad Mansoor:** Conceptualization, Formal analysis, Investigation. **Adeel Feroz Mirza:** Visualization, Data curation. **Syed Kumayl Raza Moosavi:** Validation, Formal analysis. **Filippo Sanfilippo:** Supervision, Funding acquisition, Investigation.

Declaration of Competing Interest

The authors declare that they have no known competing financial interests or personal relationships that could have appeared to influence the work reported in this paper.

References

[1] Murdock, H.E., et al., *Renewables 2020-Global status report.* 2020.
[2] Mousa HH, Youssef A-R, Mohamed EE. State of the art perturb and observe MPPT algorithms based wind energy conversion systems: a technology review. Int J Electr Power Energy Syst 2021;126:106598.
[3] Sitharthan R, Karthikeyan M, Sundar DS, Rajasekaran S. Adaptive hybrid intelligent MPPT controller to approximate effectual wind speed and optimal rotor speed of variable speed wind turbine. ISA Trans 2020;96:479–89.
[4] Breesam WI. Real-time implementation of MPPT for renewable energy systems based on Artificial intelligence. Int Trans Electrical Energy Syst 2021:e12864.
[5] Hossain MA, et al. Very short-term forecasting of wind power generation using hybrid deep learning model. J Cleaner Prod 2021;296:126564.
[6] Jiang P, Yang H, Heng J. A hybrid forecasting system based on fuzzy time series and multi-objective optimization for wind speed forecasting. Appl Energy 2019; 235:786–801.
[7] Li L-L, et al. Short-term wind power forecasting based on support vector machine with improved dragonfly algorithm. J Cleaner Prod 2020;242:118447.
[8] Alamaniotis M, Karagiannis G. Application of fuzzy multiplexing of learning Gaussian processes for the interval forecasting of wind speed. IET Renew Power Gener 2020;14(1):100–9.
[9] Zhao X, Bai M, Yang X, Liu J, Yu D, Chang J. Short-term probabilistic predictions of wind multi-parameter based on one-dimensional convolutional neural network with attention mechanism and multivariate copula distribution estimation. Energy 2021;234:121306. https://doi.org/10.1016/j.energy.2021.121306.
[10] Wan C, Wang J, Lin J, Song Y, Dong ZY. Nonparametric prediction intervals of wind power via linear programming. IEEE Trans Power Syst 2018;33(1):1074–6.
[11] Anand M, Rajapakse A, Bagen B. Stochastic model for generating synthetic hourly global horizontal solar radiation data sets based on auto regression characterization. Int Energy J 2020;20(2).
[12] Wang T, Huang S, Gao M, Wang Z. Adaptive extended Kalman filter based dynamic equivalent method of PMSG wind farm cluster. IEEE Trans Ind Appl 2021;57(3): 2908–17.
[13] Shair J, Xie X, Yuan L, Wang Y, Luo Y. Monitoring of subsynchronous oscillation in a series-compensated wind power system using an adaptive extended Kalman filter. IET Renew Power Gener 2020;14(19):4193–203.
[14] Rodríguez F, Florez-Tapia AM, Fontán L, Galarza A. Very short-term wind power density forecasting through artificial neural networks for microgrid control. Renewable Energy 2020;145:1517–27.

[15] Li L-L, et al. Using enhanced crow search algorithm optimization-extreme learning machine model to forecast short-term wind power. Expert Syst Appl 2021;184:115579.
[16] Natarajan VA, Kumari NS. Wind power forecasting using parallel random forest algorithm. In: Soft Computing for Problem Solving. Springer; 2020. p. 209–24.
[17] Haque AU, Mandal P, Meng J, Negnevitsky M. Wind speed forecast model for wind farm based on a hybrid machine learning algorithm. Int J Sustain Energ 2015;34(1):38–51.
[18] Yuan X, Chen C, Yuan Y, Huang Y, Tan Q. Short-term wind power prediction based on LSSVM–GSA model. Energy Convers Manage 2015;101:393–401.
[19] Akhter MN, et al., A Day-Ahead Power Output Forecasting of Three PV Systems Using Regression, Machine Learning and Deep Learning Techniques. 2021: AI and IOT in Renewable Energy.
[20] Liu T, Wei H, Zhang K. Wind power prediction with missing data using Gaussian process regression and multiple imputation. Appl Soft Comput 2018;71:905–16.
[21] Yan J, Ouyang T. Advanced wind power prediction based on data-driven error correction. Energy Convers Manage 2019;180:302–11.
[22] Hong Y-Y, Rioflorido CLPP. A hybrid deep learning-based neural network for 24-h ahead wind power forecasting. Appl Energy 2019;250:530–9.
[23] Zhao Y, Ye L, Li Z, Song X, Lang Y, Su J. A novel bidirectional mechanism based on time series model for wind power forecasting. Appl Energy 2016;177:793–803.
[24] Zhao, Yongning, *A novel spatio-temporal wind power forecasting framework based on multi-output support vector machine and optimization strategy*. J Clean Prod **254**.
[25] Wang C, Zhang H, Ma P. *Wind power forecasting based on singular spectrum analysis and a new hybrid Laguerre neural network*. Appl Energy 2020;259:114139. https://doi.org/10.1016/j.apenergy.2019.114139.
[26] Yu R, Gao J, Yu M, Lu W, Xu T, Zhao M, et al. LSTM-EFG for wind power forecasting based on sequential correlation features. Fut Generat Comput Syst 2019;93:33–42.
[27] Yesilbudak M, Sagiroglu S, Colak I. A novel implementation of kNN classifier based on multi-tupled meteorological input data for wind power prediction. Energy Convers Manage 2017;135:434–44.
[28] Zameer A, Arshad J, Khan A, Raja MAZ. Intelligent and robust prediction of short term wind power using genetic programming based ensemble of neural networks. Energy Convers Manage 2017;134:361–72.
[29] Liu Y, Shi J, Yang Y, Lee W-J. Short-term wind-power prediction based on wavelet transform–support vector machine and statistic-characteristics analysis. IEEE Trans Ind Appl 2012;48(4):1136–41.
[30] Devi AS, Maragatham G, Boopathi K, Rangaraj AG. Hourly day-ahead wind power forecasting with the EEMD-CSO-LSTM-EFG deep learning technique. Soft Comput 2020;24(16):12391–411.
[31] Wang Y, Wang D, Tang Y. Clustered hybrid wind power prediction model based on ARMA, PSO-SVM, and clustering methods. IEEE Access 2020;8:17071–9.
[32] Zhou B, Ma X, Luo Y, Yang D. Wind power prediction based on LSTM networks and nonparametric kernel density estimation. IEEE Access 2019;7:165279–92.
[33] Guan B et al. Spectral Domain Convolutional Neural Network. in ICASSP 2021-2021 IEEE International Conference on Acoustics, Speech and Signal Processing (ICASSP). 2021. IEEE.
[34] Specht DF. A general regression neural network. IEEE Trans Neural Networks 1991;2(6):568–76.
[35] Madhiarasan M. Accurate prediction of different forecast horizons wind speed using a recursive radial basis function neural network. Protect Control Mod Power Syst 2020;5(1):1–9.
[36] Fouad MM, El-Desouky AI, Al-Hajj R, El-Kenawy E-S. Dynamic group-based cooperative optimization algorithm. IEEE Access 2020;8:148378–403.
[37] Zafar MH, Khan UA, Khan NM. Hybrid Grey Wolf Optimizer Sine Cosine Algorithm based Maximum Power Point Tracking Control of PV Systems under Uniform Irradiance and Partial Shading Condition. IEEE; 2021.
[38] Neshat M, et al. Wind turbine power output prediction using a new hybrid neuro-evolutionary method. Energy 2021;229:120617.
[39] Zafar MH, et al. Bio-inspired optimization algorithms based maximum power point tracking technique for photovoltaic systems under partial shading and complex partial shading conditions. J Cleaner Prod 2021;309:127279.
[40] Hao Y, Tian C. A novel two-stage forecasting model based on error factor and ensemble method for multi-step wind power forecasting. Appl Energy 2019;238:368–83.